Solitary wave propagation and steering through light-induced refractive potentials

Gaetano Assanto,[1] Benjamin D. Skuse,[2] and Noel F. Smyth[2]

[1]*NooEL—Nonlinear Optics and OptoElectronics Laboratory, Department of Electronic Engineering, INFN–CNISM–University of Rome "Roma Tre," Via della Vasca Navale 84, I-00146 Rome, Italy*

[2]*School of Mathematics and Maxwell Institute for Mathematical Sciences, The King's Buildings, University of Edinburgh, Edinburgh EH9 3JZ, Scotland, United Kingdom*

(Received 16 March 2010; published 10 June 2010)

The steering of a self-guided beam in a dye-doped nematic liquid crystal caused by an external illumination (control beam) that induces changes in the refractive index of the medium is theoretically analyzed. The interaction between the control beam and the dye molecules modifies the anchoring of the nematic molecules, so changing the director orientation in the bulk of the medium. Beam evolution is investigated by use of a modulation theory approach. It is found that the beam trajectory is independent of the beam profile, as long as this profile is self-similar. Solutions obtained from the modulation theory approach are in excellent agreement with numerical solutions.

DOI: 10.1103/PhysRevA.81.063811 PACS number(s): 42.65.Tg, 42.70.Df

I. INTRODUCTION

Numerous articles on experimental as well as theoretical aspects of the propagation of nematicons, that is, optical spatial solitary waves in nematic liquid crystals (NLCs), reveal the growing interest in self-localized light beams in reorientationally nonlinear media [1–10]. Some of the most striking results reported on nematicons concern their propagation through interfaces between liquid-crystalline regions that differ in refractive index and birefringence, including positive and negative refraction, as well as total internal reflection [11–16]. Among the latest findings, refraction and total internal reflection of nematicons were demonstrated in a dye-doped NLC illuminated by external beams at a wavelength absorbed by the dye, that is, the introduction of all-optically-induced graded interfaces along the soliton path [17]. Here all-optical steering of self-localized beams in dye-doped nematic liquid crystals using an averaged Lagrangian method is theoretically addressed, resulting in modulation equations for the solitary wave parameters. Polarizations of the external beam resulting in both increased and decreased refractive index under the illuminated region are considered. It is found that, in the nonlocal regime appropriate to the problem [18], the nematicon trajectory is independent of its functional form. This independence of the nematicon trajectory of the profile of the nematicon results in excellent agreement between this trajectory as given by the modulation equations and numerical solutions, with errors generally less than 0.1%, but never exceeding around 1%. In addition, the nematicon amplitudes as given by modulation theory and by numerical solutions are in excellent agreement. This excellent prediction of the soliton paths in light-perturbed NLCs by use of modulation theory is expected to hold in other situations for which nematicons undergo interactions with pointwise refractive index changes, as reported in previous experiments [19–23].

II. MODULATION THEORY

Let us consider the propagation of coherent, polarized light through a cell containing a nematic liquid crystal, in which a separate light beam is shone into the cell in the direction x orthogonal to the cell boundaries, as illustrated in Fig. 1. An external static or low-frequency electric field is applied to pretilt the nematic director (or optic axis) in the xz plane at an angle $\hat{\theta}$ to the direction z in order to overcome the Fréedericksz transition threshold [1]. The coordinates (x, y) are orthogonal to z. The NLC is doped with a small amount ($\sim$1%) of a photosensitive dye absorbing light in a given spectral region. If an external control beam (illumination beam) of a wavelength appropriate for dye absorption is shone into the cell, the dye molecules collect external energy. Molecules near the (upper and lower) interfaces defining the cell provide the anchoring of the NLC director at the boundaries, and the light-driven excitation of the dye molecules can alter the alignment of and, because of intermolecular forces, modify the layout of the NLC optic axis in the whole volume under the illuminated region [24,25]. Stated in another way, the external illumination of the cell with a dye-doped NLC can reorient the underlying medium and modify its linear and nonlinear properties through the distribution of its optic axis [26]. Let us assume that the illumination beam is one dimensional and is shone into the nematic cell between z_1 and z_2, as illustrated in Fig. 1. The resulting perturbation of the director angle from the pretilt $\hat{\theta}$ is θ_b.

With this externally induced light perturbation, let us now consider an x-polarized beam (extraordinary wave) launched with wave vector in the plane yz of the cell and with a wavelength outside the absorption band of the dye. The Poynting vector of this input beam initially propagates with respect to z at an angle being a combination of the input angle and the birefringent walk-off. Let θ_n be the perturbation of the molecular director distribution owing to the nonlinear response of the NLC to this light beam (nematicon).

To model the interaction between these two beams, one freely propagating in the nonlinear medium and the other absorbed by the dye, let us first consider the external beam. In the experiments reported by Piccardi and co-workers [17], the control beam had a highly elliptical cross section. This illumination can be approximated as an infinitely extended stripe along y of uniform intensity and finite width along z. The equation governing the resulting director angle perturbation θ_b is then [5]

$$\nu \frac{\partial^2 \theta_b}{\partial z^2} - 2q\theta_b = 2p|E_b|^2, \tag{1}$$

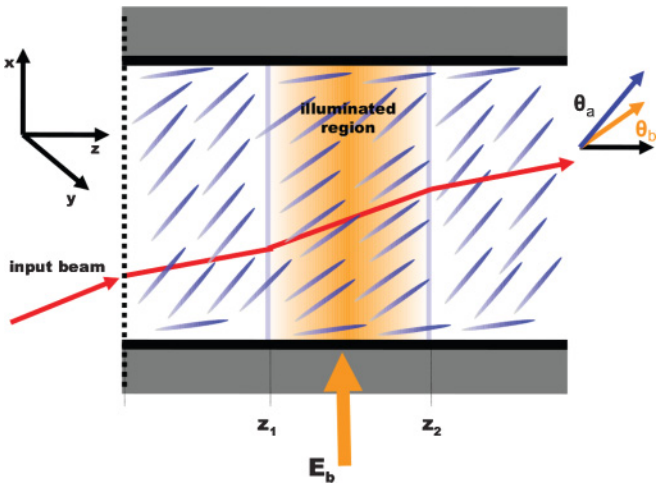

FIG. 1. (Color online) Sketch of a dye-doped nematic liquid-crystal cell with an externally illuminated region. The red line represents a nematicon with a curved trajectory caused by the nonuniform index and optic axis distribution induced by the external beam.

where E_b is the electric field envelope of the illumination beam, q is related to the square of the voltage bias, and ν measures the nonlocality of the medium, with large ν corresponding to a highly nonlocal response. As the latter applies in most experimental cases, ν will be taken large [18]. This director equation, and all subsequent equations, are in nondimensional form. Depending on the polarization of the illumination beam, the resulting reorientation of the NLC can cause a decrease ($p = 1$) or an increase ($p = -1$) in the refractive index for extraordinarily polarized waves. For the stripe, E_b is given by

$$E_b = \begin{cases} E_0 & \text{if } z_1 < z < z_2, \\ 0 & \text{otherwise.} \end{cases} \tag{2}$$

With this external beam distribution, the director equation (1) in xz has the solution

$$\theta_b = F(z)e^{-\gamma x} = \begin{cases} pA_1 e^{\kappa z - \gamma x}, & z < z_1, \\ p\left(A_2 e^{-\kappa z} + A_3 e^{\kappa z} - \dfrac{|E_0|^2}{q}\right) e^{-\gamma x}, & z_1 \leqslant z \leqslant z_2, \\ pA_4 e^{-\kappa z - \gamma x}, & z > z_2, \end{cases} \tag{3}$$

where $\kappa = \sqrt{2q/\nu}$ and

$$A_1 = \frac{|E_0|^2}{2q}(e^{-\kappa z_2} - e^{-\kappa z_1}),$$
$$A_2 = \frac{|E_0|^2}{2q}e^{\kappa z_1}, \quad A_3 = \frac{|E_0|^2}{2q}e^{-\kappa z_2}, \tag{4}$$
$$A_4 = \frac{|E_0|^2}{2q}(e^{\kappa z_1} - e^{\kappa z_2}).$$

This is the director environment in which the nematicon beam propagates. As the illumination beam propagates across the cell, it undergoes absorption and scattering losses [17]. If we assume that this loss is linear, the illumination beam then gains an exponential decay in x, so that the exponential factor $e^{-\gamma x}$ has been added to the solution (3) [27]. In addition to this attenuation, the illumination beam experiences diffractive spreading in x [17]. This spreading has been neglected so that relatively simple modulation equations can be derived. The inclusion of realistic spreading across the NLC thickness would greatly increase the complexity of the calculations.

With the illumination beam setting up a refractive index profile in the medium, a self-localized nonlinear wave (a nematicon) can now be introduced. This is taken to propagate in the xz plane. Its trajectory will undergo refraction because of the perturbation induced on the director angle by the control beam. The electric field envelope of this nematicon is denoted E_n, and the change in the director angle produced by the nematicon is θ_n. The equations governing the nematicon can then be cast as [5,16,28]

$$i\frac{\partial E_n}{\partial z} + \frac{1}{2}\nabla^2 E_n + 2E_n(\theta_n + \theta_b) = 0, \tag{5}$$
$$\nu\nabla^2\theta_n - 2q\theta_n = -2|E_n|^2, \tag{6}$$

with the Laplacian ∇^2 in the xy plane. For a nematicon to exist, it must compensate diffraction via self-focusing, that is, produce an increase in refractive index, which is why $|E_n|^2$ has a negative sign in Eq. (6). The director perturbation θ_b produced by the external beam does not appear in the director equation (6) because the latter is linear, and the control beam perturbation satisfies Eq. (1). This is justified by the fact that, in the paraxial approximation, θ_n does not depend directly on z. As the electric field equation is nonlinear, the director perturbation θ_b because of the illumination beam appears in Eq. (5). The term $2E_n\theta_b$ acts as a refractive index inhomogeneity which curves the nematicon trajectory. A similar inhomogeneity was also found in the waveguide owing to an applied electric field [16].

The nematicon equations (5) and (6) have no exact solution, even in the absence of an illumination beam. A useful approximate method of solution in this case is based on the use of trial functions in an averaged Lagrangian formulation of the nematicon equations [7,16,29]. In previous cases it was necessary to assume a form for the nematicon profile, but here the nematicon profile will be left arbitrary. Appropriate trial functions for the electric field E_n of the nematicon and the director perturbation θ_n caused by self-focusing are then

$$E_n = af(\chi/w)\,e^{i\psi} + ige^{i\psi}, \quad \theta_n = \alpha f^2(\chi/\beta), \tag{7}$$

where

$$\chi = \sqrt{(x-\xi)^2 + y^2}, \quad \psi = \sigma + \Phi(x - \xi). \tag{8}$$

The electric field amplitude a, width w, director perturbation amplitude α and width β, nematicon position ξ, propagation angle Φ, phase σ, and shelf amplitude g are functions of z. The first term in the trial function for E_n is a solitary wave with variable parameters. The second term represents the out-of-phase interaction of the nematicon with a flat shelf of low-amplitude diffractive radiation which develops under the evolving beam and travels with it [7,28,29]. If the shelf were assumed to have nonzero amplitude throughout the bulk medium, then the mass of the shelf would be infinite; hence, the shelf is assumed to be a disk of radius R, so that g is nonzero

in $0 \leqslant \chi \leqslant R$ [7,28,29]. The nematicon profile, given by f, is a self-similar, but as yet unspecified, functional form $f(\rho)$, simply requiring that $f(\rho)$ decays fast enough as $\rho \to \pm\infty$ so that the resulting integrals in the modulation equations converge. The nematicon's transverse profile is left arbitrary because its position will be found to be independent of the exact form of f. For the numerical comparisons presented below, hyperbolic secant $\operatorname{sech}\rho$ and Gaussian $e^{-\rho^2}$ profiles were used as specific examples.

The nematicon equations (5) and (6) have the Lagrangian formulation

$$L = i\left(E_n^*\frac{\partial E_n}{\partial z} - E_n\frac{\partial E_n^*}{\partial z}\right) - |\nabla E_n|^2 + 4(\theta_n+\theta_b)|E_n|^2 - \nu|\nabla\theta_n|^2 - 2q\theta_n^2, \tag{9}$$

with the asterisk denoting the complex conjugate. The averaged Lagrangian $\mathcal{L}$ is calculated by substitution of the trial functions (7) into this Lagrangian and integration in x and y from $-\infty$ to ∞ [30]. In a similar manner to that used in previous work [7], this yields

$$\mathcal{L} = -2(a^2w^2I_2 + \Lambda g^2)\left(\frac{d\sigma}{dz} - \Phi\frac{d\xi}{dz}\right) - 2I_1aw^2\frac{dg}{dz} + 2I_1gw^2\frac{da}{dz} + 4I_1awg\frac{dw}{dz} - a^2I_{22} - (a^2w^2I_2 + \Lambda g^2)\Phi^2 - 4\nu I_{42}\alpha^2 - 2qI_4\alpha^2\beta^2 + \frac{2A^2B^2\alpha a^2\beta^2w^2}{A^2\beta^2 + B^2w^2} + 2F(z)a^2B^2w^2e^{-\gamma\xi+\gamma^2B^2w^2/4}. \tag{10}$$

The modulation equations for the nematicon parameters are then the variational equations of this averaged Lagrangian. These modulation equations are

$$\frac{d}{dz}(I_2a^2w^2 + \Lambda g^2) = 0, \tag{11}$$

$$\frac{d}{dz}(I_1aw^2) = \Lambda g\left(\frac{d\sigma}{dz} - \frac{1}{2}\Phi^2\right), \tag{12}$$

$$I_1\frac{dg}{dz} = \frac{I_{22}a}{2w^2} - \frac{A^2B^4aw^2\alpha\beta^2}{(A^2\beta^2 + B^2w^2)^2} + \frac{1}{4}F(z)\gamma^2B^4aw^2e^{-\gamma\xi+\gamma^2B^2w^2/4}, \tag{13}$$

$$I_2\left(\frac{d\sigma}{dz} - \frac{1}{2}\Phi^2\right) = -\frac{I_{22}}{w^2} + \frac{A^2B^2\alpha\beta^2(A^2\beta^2 + 2B^2w^2)}{(A^2\beta^2 + B^2w^2)^2} + F(z)B^2\left(1 - \frac{\gamma^2B^2w^2}{4}\right)e^{-\gamma\xi+\gamma^2B^2w^2/4}, \tag{14}$$

$$\frac{d}{dz}[(I_2a^2w^2 + \Lambda g^2)\Phi] = -2I_2F(z)\gamma a^2w^2e^{-\gamma\xi+\gamma^2B^2w^2/4}, \tag{15}$$

$$\frac{d\xi}{dz} = \Phi, \tag{16}$$

with the algebraic equations

$$\alpha = \frac{A^2B^4a^2w^4}{qI_4(A^2\beta^2 + B^2w^2)^2}, \qquad \alpha = \frac{A^2B^2a^2\beta^2w^2}{(A^2\beta^2 + B^2w^2)(4\nu I_{42} + 2qI_4\beta^2)}. \tag{17}$$

The various integrals I_i and I_{ij} and the constants A and B are given in the Appendix. Owing to the short propagation lengths considered here, these equations do not include the dissipative effect of the diffractive radiation shed by the nematicon as it evolves [7]. Solutions of these modulation equations will now be compared with full numerical solutions of the nematicon equations. The field equation (5) was solved using a pseudospectral method similar to that of Fornberg and Whitham [31]. The director equation (6) was solved as a boundary value problem using a Fourier method [32]. The numerical method is the same as that of Skuse and Smyth [33], so no further description will be given here. The modulation equations were solved using the standard fourth-order Runge-Kutta scheme.

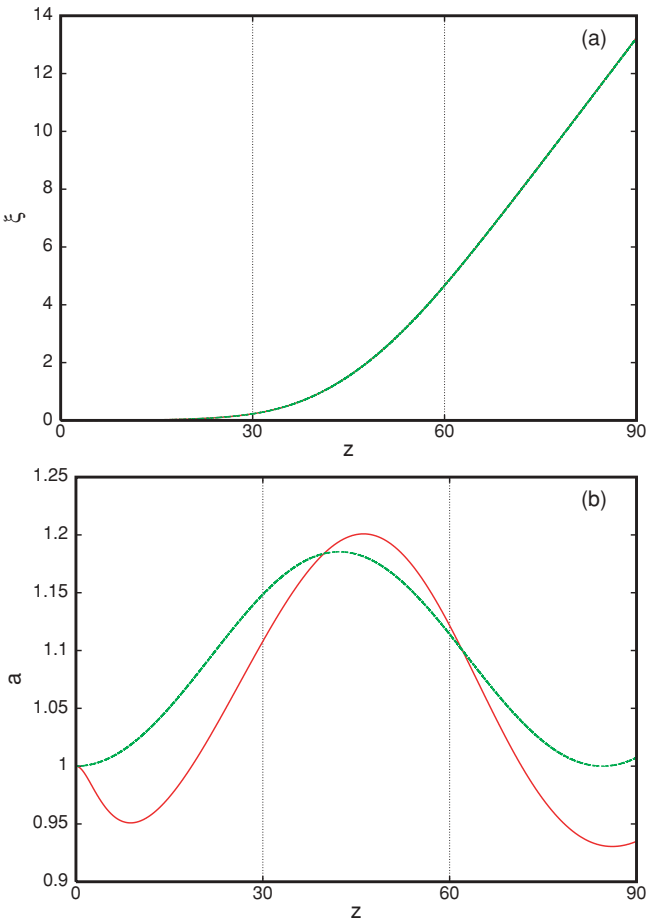

FIG. 2. (Color online) Comparisons for an optically rarer (lower-index) region ($p = 1$) for the initial conditions $a = 1.0$, $w = 3.5$, $\Phi_0 = 0.0$, $\xi = 0.0$, $E_0 = 1.0$, $\gamma = 0.01$, $\nu = 200$, and $q = 2$ with $z_1 = 30$ and $z_2 = 60$ for $f(\rho) = \operatorname{sech}\rho$. Full numerical solution (—) (red); solution of modulation equations (– – –) (green). (a) Positions; (b) amplitudes.

III. COMPARISON WITH NUMERICAL RESULTS

A comparison between a full numerical solution and a modulation solution for (a) the peak position and (b) the amplitude of the solitary beam is presented in Fig. 2 for an optically rarer region, that is, a defect with a lower refractive index ($p = 1$). The choice $f(\rho) = \operatorname{sech}\rho$ was made for the trial function, with the initial numerical profile of the same form. It can be seen that there is perfect agreement for the beam position, with excellent agreement for the amplitude evolution. The beam is seen to refract before it enters the illuminated region in $30 < z < 60$. This is because of the nonlocal nature of the NLC response, so that the external beam causes reorientation of the nematic liquid-crystal director well outside the illuminated region, as seen from the solution (3) for the control-induced reorientation θ_b of the director.

The nearly perfect agreement between the modulation and numerical solutions for the position of the nematicon is verified over the full range of input angles Φ_0, as can be seen from Fig. 3. This figure shows the angle of refraction of the nematicon as a function of its input angle for an optically rarer region, $p = 1$. The angle of refraction is calculated as the angle the soliton makes with respect to z in the xz plane when it has propagated far from the illuminated region. The percentage error in the predictions of the modulation theory as compared with the numerical solutions is generally well below 1% and typically around 0.1% for most of the range of Φ_0. This agreement is a substantial improvement over the 1%–2% agreement for the nematicon position in previous studies of the interaction between two-color nematicons; for example, [33,34]. The reason for such a good agreement can be found by studying the role of various nematicon profiles.

Figure 4 shows a comparison of the nematicon amplitude and position as given by the numerical solution for two initial profiles, namely, a sech $[f(\rho) = \operatorname{sech}\rho]$ and a Gaussian $[f(\rho) = \exp(-\rho^2)]$. The initial amplitudes and widths for the sech and Gaussian profiles were chosen to be different, with no attempt made to fit the Gaussian to the sech profile. Clearly, the amplitude evolutions for the two profiles are widely different. However, the position evolutions are identical within graphic accuracy. For the nonlocal parameters chosen

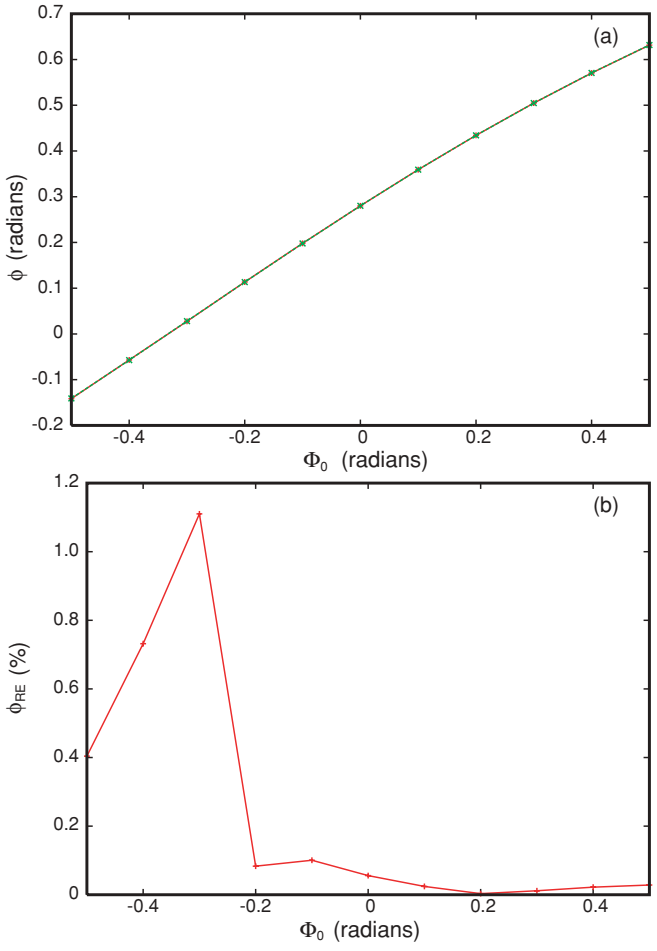

FIG. 3. (Color online) (a) Refraction angle as given by the full numerical solutions (—+—) (red) and the modulation solutions (– –×– –) (green) and (b) refraction angle percentage error ϕ_{RE} through an optically rarer index region ($p = 1$) for $f(\rho) = \operatorname{sech}\rho$ as given by the modulation solutions relative to the numerical solutions as a function of Φ_0 with initial values $a = 1.0$, $w = 3.5$, $\xi = 0.0$, $E_0 = 1.0$, $\gamma = 0.01$, $\nu = 200$, $q = 2$, where $z_1 = 30$, $z_2 = 60$.

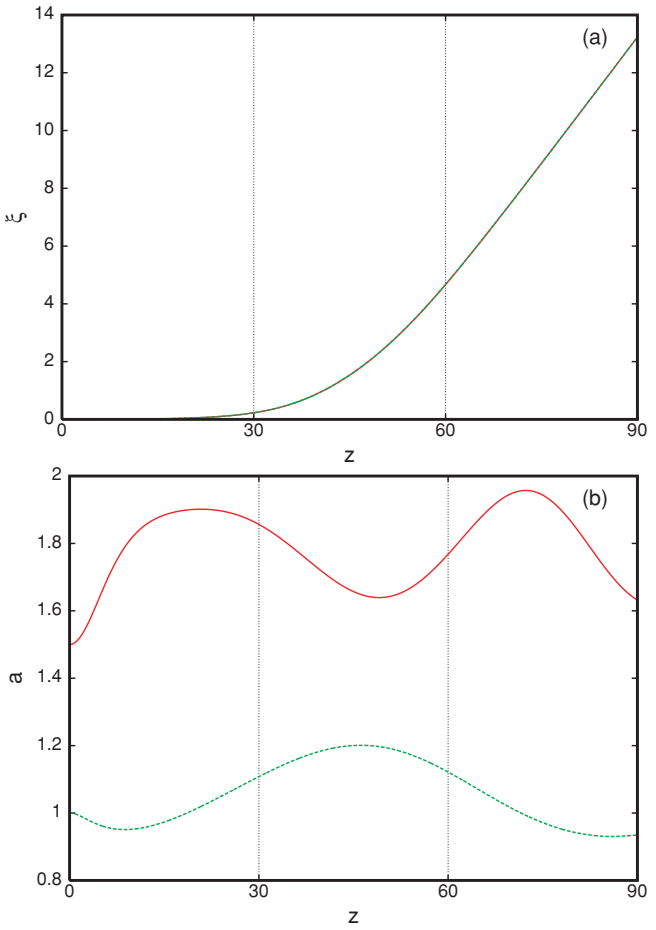

FIG. 4. (Color online) Full numerical solutions with initial values $\Phi_0 = 0.02$, $\xi = 0.0$, $E_0 = 1.5$, $\gamma = 0.01$, $\nu = 200$, and $q = 2$ with $z_1 = 30$ and $z_2 = 60$ for an optically rarer region ($p = 1$) for $f(\rho) = \operatorname{sech}\rho$ with $a = 1.0$, $w = 3.5$ (—) (red) and for a Gaussian initial profile $f(\rho) = \exp(-\rho^2)$ with $a = 1.5$, $w = 5$ (– – –) (green). (a) Positions; (b) amplitudes.

in the current study, the modulation equations (11)–(16) predict such insensitivity to the beam profile. In the nonlocal regime, the amount of radiation shed by the nematicon as it propagates is small, so that g is small [7]. The Λg^2 term in the momentum equation (15) is then negligible and the profile factor $I_2 a^2 w^2$ cancels out. Furthermore, the decay rate γ was chosen to be small, as in the experimental report [17], so that the term $\gamma^2 B^2 w^2/4$ in the exponent on the right-hand side of the momentum equation (15) is negligible compared to $-\gamma\xi$. Hence, in the nonlocal limit with a small decay of the illumination beam, any contributions of the specific nematicon profile cancel out of the momentum equation (15) and the beam trajectory is independent of the transverse shape of the beam, as long as it is self-similar. The latter is confirmed by the numerical trajectory being independent of the profile. The modulation solution assumes that the nematicon retains its initial shape. While the numerical profile evolves from its initial form, the independence of the trajectory of the soliton profile still allows near-perfect agreement between the numerical and modulation trajectories. However, the details of the nematicon profile do not cancel out of the amplitude equation (12) under the nonlocal and small-γ assumptions. Therefore the amplitude evolution will depend on the nematicon profile, consistent with Fig. 4(b).

The excellent agreement between the numerical and modulation solutions also holds for an optically denser (higher-index) region, so that $p = -1$. The independence of the nematicon trajectory of the details of its profile in the nonlocal limit with modest decay of the illumination beam γ will still hold as the canceling out of all details of the profile from the momentum equation (15) is independent of the polarization of the illumination beam. Figure 5 shows comparisons of the refraction angle and the percentage error in it as given by the numerical and modulation solutions, but as a function of the intensity of the illumination beam. The agreement is again excellent, with some deviation for higher powers. Overall the agreement is similar to that shown in Fig. 3 for a less dense illuminated region.

The reason for the deviation between the numerical and modulation solutions for high control beam intensity when the illuminated region is optically denser can be seen in a specific example with $E_0 = 1.5$, as shown in Fig. 6. After the nematicon has left the illuminated region, oscillations

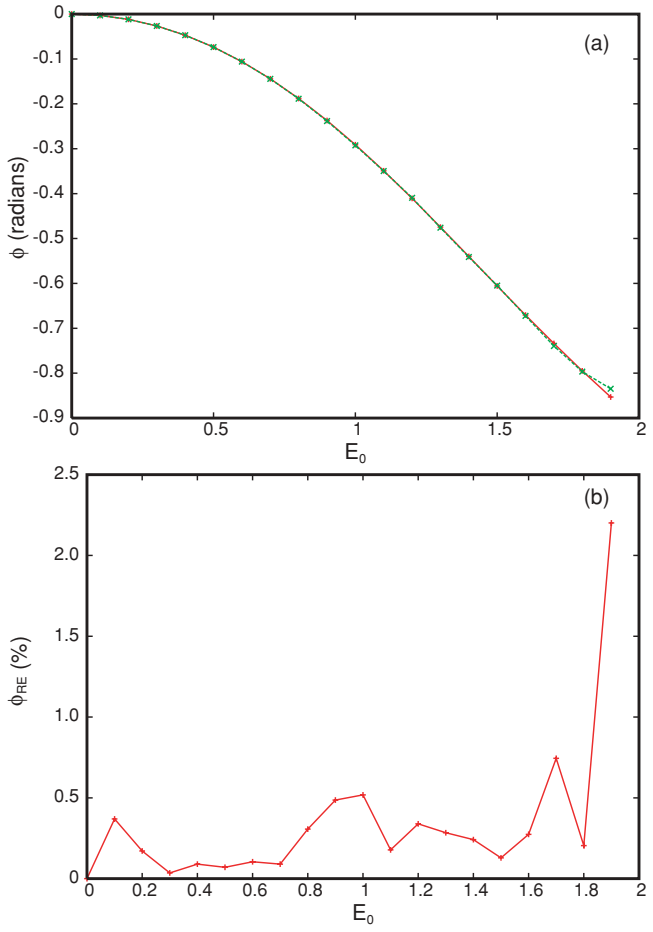

FIG. 5. (Color online) (a) Refraction angle ϕ as given by the full numerical solutions (—+—) (red) and the modulation solutions (– –×– –) (green) and (b) angle of refraction percentage error ϕ_{RE} through an optically denser region ($p = -1$) as given by the modulation solutions relative to the numerical solutions for $f(\rho) =$ sech ρ as a function of E_0 with initial values $a = 1.0$, $w = 3.5$, $\xi = 0.0$, $\Phi_0 = 0.0$, $\gamma = 0.01$, $\nu = 200$, $q = 2$, where $z_1 = 30$, $z_2 = 60$.

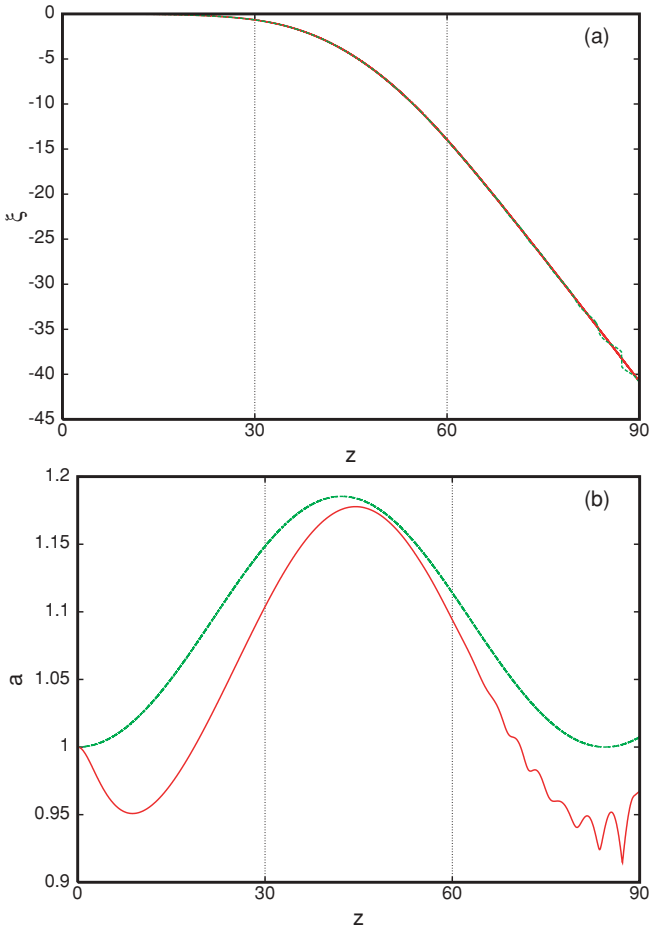

FIG. 6. (Color online) Comparisons for the initial values $a = 1.0$, $w = 3.5$, $\Phi_0 = 0.0$, $\xi = 0.0$, $E_0 = 1.5$, $\gamma = 0.01$, $\nu = 200$, and $q = 2$ where $z_1 = 30$ and $z_2 = 60$ for an optically denser region ($p = -1$) with a sech initial profile. Full numerical solution (—) (red); modulation solution (– – –) (green). (a) Positions; (b) amplitudes.

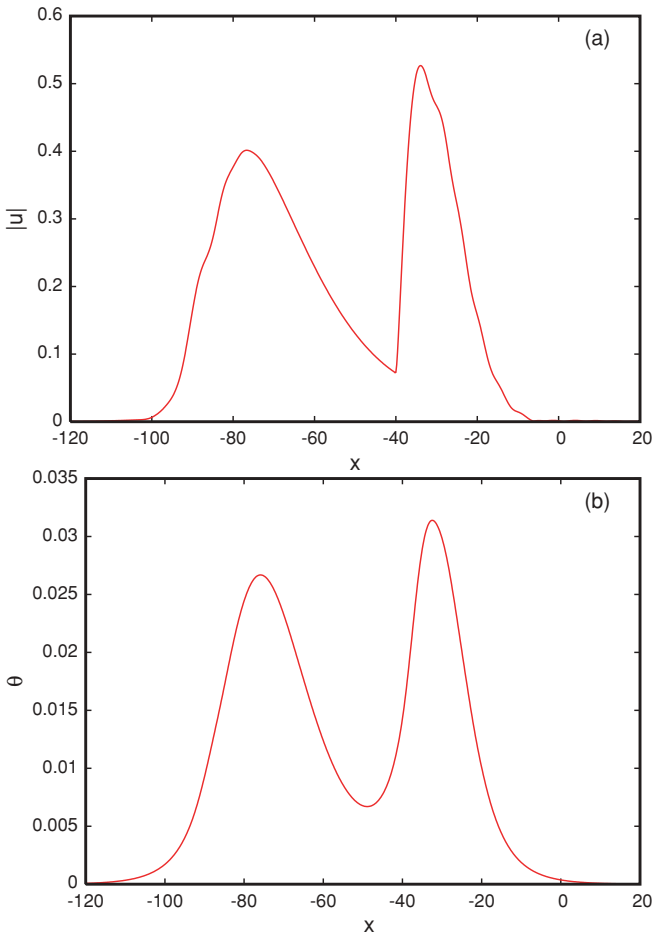

FIG. 7. (Color online) Full numerical solution for a sech initial profile at $z = 57$ with initial values $a = 1.0$, $w = 3.5$, $\Phi_0 = -1.0$, $\xi = 0.0$, $E_0 = 1.5$, $\gamma = 0.01$, $\nu = 200$, and $q = 2$ where $z_1 = 30$ and $z_2 = 60$ for an optically denser region ($p = -1$). (a) Solution for $|u|$; (b) solution for θ.

appear in the numerical position and amplitude as the soliton breaks up into two beams. As the nematicon refracts into a region with a higher illumination intensity, as can be seen from Fig. 6(a), the director perturbation θ_b owing to illumination increases, so that the nonlinear coefficient in the nonlinear-Schrödinger-type equation (5) increases as well. If this nonlinearity grows enough, an individual nematicon will break up into multiple nematicons, as expected from standard solitary wave theory [30]. The numerical solution shows oscillations in the amplitude and position as the code seeks the location of the maximum of $|E_n|$ in order to determine the position of the nematicon. The oscillations are therefore due to the code "hopping" between the two generated solitons as each in turn has a higher amplitude. This generation of multiple nematicons for high illumination intensity is illustrated in Fig. 7. For the higher input angle used, the nematicon has split into two inside the defect region.

IV. CONCLUSIONS

The propagation of a solitary wave, a nematicon, through a bulk nematic liquid crystal in the presence of an index of refraction variation caused by a localized illumination beam has been modeled by use of a variational technique. Its predictions have been found to be in excellent agreement with numerical solutions of the governing equations. The rather surprising result of the analysis is that, in the nonlocal response regime, the nematicon trajectory is independent of its transverse profile, as long as it is self-similar.

The independence of the nematicon trajectory of the specifics of its profile should extend to other situations in which a nematicon is refracted through changes in the refractive index owing to variations in the director orientation, whether these are due to other beams or to the applied voltage. One of the problems with modeling nonlinear wave evolution in higher dimensions has been the lack of an exact steady solitary wave (nematicon) solution on which to base perturbation theory, or other types of analytical analysis. The present finding—that this knowledge is not necessary for a localized index variation—allows the inference that the same independence from the profile shape should apply to other problems of accessible solitons [5,35] propagating through refractive perturbations.

ACKNOWLEDGMENTS

This research was supported by the Royal Society of London under Grant No. JP090179.

APPENDIX: INTEGRALS

The integrals I_i and $I_{i,j}$ in the modulation equations are

$$I_1 = \int_0^\infty \rho f(\rho)\, d\rho, \quad I_2 = \int_0^\infty \rho f^2(\rho)\, d\rho,$$
$$I_{22} = \int_0^\infty \rho \left(\frac{df}{d\rho}\right)^2 d\rho, \quad I_{x32} = \int_0^\infty \rho^3 f^2(\rho)\, d\rho, \qquad \text{(A1)}$$
$$I_{42} = \frac{1}{4}\int_0^\infty \rho \left(\frac{d}{d\rho} f^2(\rho)\right)^2 d\rho,$$
$$I_4 = \int_0^\infty \rho f^4(\rho)\, d\rho.$$

The constants A and B arising in the modulation equations are

$$A = \frac{I_2\sqrt{2}}{\sqrt{I_{x32}}} \quad \text{and} \quad B = \sqrt{2I_2}. \qquad \text{(A2)}$$

[1] M. Peccianti, G. Assanto, A. De Luca, C. Umeton, and I. C. Khoo, Appl. Phys. Lett. **77**, 7 (2000).
[2] M. Peccianti and G. Assanto, Opt. Lett. **26**, 1690 (2001).
[3] M. Peccianti and G. Assanto, Phys. Rev. E **65**, 035603(R) (2002).
[4] G. Assanto, M. Peccianti, and C. Conti, Opt. Photonics News, **14**, 44 (2003).

[5] C. Conti, M. Peccianti, and G. Assanto, Phys. Rev. Lett. **91**, 073901 (2003).
[6] M. Peccianti, C. Conti, G. Assanto, A. De Luca, and C. Umeton, Nature (London) **432**, 733 (2004).
[7] A. A. Minzoni, N. F. Smyth, and A. L. Worthy, J. Opt. Soc. Am. B **24**, 1549 (2007).
[8] G. Assanto, N. F. Smyth, and A. L. Worthy, Phys. Rev. A **78**, 013832 (2008).
[9] A. Alberucci, G. Assanto, D. Buccoliero, A. S. Desyatnikov, T. R. Marchant, and N. F. Smyth, Phys. Rev. A **79**, 043816 (2009).
[10] G. Assanto, A. Minzoni, and N. F. Smyth, J. Nonlinear Opt. Phys. Mater. **18**, 1 (2009).
[11] M. Peccianti, A. Dyadyusha, M. Kaczmarek, and G. Assanto, Nature Phys. **2**, 737 (2006).
[12] M. Peccianti, G. Assanto, A. Dyadyusha, and M. Kaczmarek, Phys. Rev. Lett. **98**, 113902 (2007).
[13] M. Peccianti, G. Assanto, A. Dyadyusha, and M. Kaczmarek, Opt. Lett. **32**, 271 (2007).
[14] M. Peccianti and G. Assanto, Opt. Express **15**, 8021 (2007).
[15] M. Peccianti, A. Dyadyusha, M. Kaczmarek, and G. Assanto, Phys. Rev. Lett. **101**, 153902 (2008).
[16] G. Assanto, A. A. Minzoni, M. Peccianti, and N. F. Smyth, Phys. Rev. A **79**, 033837 (2009).
[17] A. Piccardi, G. Assanto, L. Lucchetti, and F. Simoni, Appl. Phys. Lett. **93**, 171104 (2008).
[18] C. Conti, M. Peccianti, and G. Assanto, Phys. Rev. Lett. **92**, 113902 (2004).
[19] A. Pasquazi, A. Alberucci, M. Peccianti, and G. Assanto, Appl. Phys. Lett. **87**, 261104 (2005).
[20] S. V. Serak, N. V. Tabiryan, M. Peccianti, and G. Assanto, IEEE Photonics Technol. Lett. **18**, 1287 (2006).
[21] A. Alberucci, A. Piccardi, U. Bortolozzo, S. Residori, and G. Assanto, Opt. Lett. **35**, 390 (2010).
[22] A. Piccardi, A. Alberucci, U. Bortolozzo, S. Residori, and G. Assanto, Appl. Phys. Lett. **96**, 071104 (2010).
[23] A. Piccardi, A. Alberucci, U. Bortolozzo, S. Residori, and G. Assanto, Photon. Techn. Lett. **22**, 694 (2010).
[24] F. Simoni, L. Lucchetti, D. Lucchetta, and O. Francescangeli, Opt. Express **9**, 85 (2001).
[25] L. Lucchetti, M. Gentili, and F. Simoni, Opt. Express **14**, 2236 (2006).
[26] M. Peccianti, C. Conti, and G. Assanto, Opt. Lett. **30**, 415 (2005).
[27] Yu. S. Kivshar and G. Agrawal, *Optical Solitons: From Fibers to Photonic Crystals* (Academic Press, San Diego, 2003).
[28] C. García-Reimbert, A. A. Minzoni, and N. F. Smyth, J. Opt. Soc. Am. B **23**, 294 (2006).
[29] W. L. Kath and N. F. Smyth, Phys. Rev. E **51**, 1484 (1995).
[30] G. B. Whitham, *Linear and Nonlinear Waves* (J. Wiley and Sons, New York, 1974).
[31] B. Fornberg and G. B. Whitham, Philos. Trans. R. Soc. London, Ser. A **289**, 373 (1978).
[32] W. H. Press, S. A. Teukolsky, W. T. Vetterling, and B. P. Flannery, *Numerical Recipes in Fortran. The Art of Scientific Computing* (Cambridge University Press, Cambridge, 1992).
[33] B. D. Skuse and N. F. Smyth, Phys. Rev. A **77**, 013817 (2008).
[34] B. D. Skuse and N. F. Smyth, Phys. Rev. A **79**, 063806 (2009).
[35] A. W. Snyder and M. J. Mitchell, Science **276**, 1538 (1997).